

Digital Implementation and Transient Simulation of Space-Vector Modulated Converters

A. Mehrizi-Sani, *Student Member, IEEE*, and S. Filizadeh, *Member, IEEE*

Abstract—Voltage-source converters (VSCs) are building blocks of high-power electronic apparatus used in modern power networks. Pulse-width modulation is used widely for the synthesis of ac voltages at the terminals of a VSC. A powerful alternative for this purpose is the space-vector modulation, in which the converter is placed in a finite number of known states in order to best approximate the reference voltage. This method offers better utilization of the dc bus voltage and provides several degrees of freedom for enhancement of the harmonic spectrum. The paper presents a digital implementation of the technique in a transient simulation program (PSCAD/EMTDC). The developed model, which covers both linear and nonlinear modes of operation, is very useful in the design and analysis of modern power networks (and drive systems) with embedded power electronics, and also allows comprehensive harmonic analysis to be conducted. The usefulness of the method is demonstrated through an example.

Index Terms— Harmonic spectrum, space-vector modulation, transient simulation, voltage-source converters.

I. INTRODUCTION

HIGH-power electronic converters are known to provide convenient means for the regulation of real and reactive power flow, voltage support, and improvement of dynamic performance of power networks. Use of such converters, in particular voltage-source converters (VSCs), within the context of modern power systems has been accelerated with the advent of fast switching devices with higher ratings as well as development of advanced techniques for their control.

The output voltage of a VSC comprises a number of $\pm V_{dc}/2$ voltage pulses (in a two-level VSC with a dc link voltage of V_{dc}). Pulse-width modulation (PWM) techniques are used to design the width of such pulse sequences so that a fundamental component voltage with specified magnitude and phase emerges, and harmonics are shifted towards higher frequency bands. Such techniques are applied essentially independently for the three phases.

An alternative method, which has attracted a great deal of attention since its introduction, is the space-vector modulation (SVM) technique [1], [2]. In this method the converter is

treated as single unit, which can assume a finite number of states depending on the combination of the states of its controlled switches. In a two-level converter, these combinations result in six active (non-zero) states and two zero states. In digital implementation of the SVM the aim is to find an appropriate combination of active and zero vectors so that the reference space vector (which represents the reference voltage) is best approximated.

Since SVM provides a great deal of flexibility in determination of the share of zero space vectors as well as the sequence of appropriate active space vectors, a large collection of implementation methods, both in linear and in overmodulation ranges, becomes possible. As long as operation in linear region is concerned, however, all SVM strategies produce a line voltage for which the fundamental component magnitude increases linearly with modulation index. Modulation strategies in the linear region are generally different in the way they treat zero vectors [3], the number of samples in each sector [4], [5], and the sequence of active vector placement [6]. On the other hand, different overmodulation approaches treat the transition from linear operation to square-wave operation in nonlinear range differently.

In this paper, a digital implementation of the SVM technique in the PSCAD/EMTDC electromagnetic transient simulation program is presented. Electromagnetic transient simulation programs are standard tools for the study of short-term, transient phenomena in power systems. Power electronic circuits embedded in modern power networks extensively use VSCs as their building blocks. Rapid switchings in these circuits generate harmonics and transients that could be best modeled, simulated and analyzed using a transient simulation program. As such it is important to develop models for various firing pulse generation schemes in these programs.

The model developed here generates firing pulses for a VSC for the entire range of operation, from linear mode to overmodulation. The model can be used in detailed simulations of power systems or industrial drives that use SVM techniques for voltage synthesis using VSCs. It also produces valuable information that could be used subsequently for harmonic spectrum studies. The paper describes, in detail, the mathematical foundations of the SVM technique and over-

A. Mehrizi-Sani and S. Filizadeh are with the Department of Electrical and Computer Engineering, University of Manitoba, Winnipeg, MB, Canada (email: mehrizi@ee.umanitoba.ca, sfilizad@ee.umanitoba.ca).

modulation variations. It also describes the implementation in PSCAD/EMTDC. Various simulation results to show validity of the model conclude the paper.

II. BASICS OF SPACE VECTOR MODULATION

Conventional sinusoidal pulse-width modulation essentially compares a low-frequency sinusoid with a high frequency triangular or saw-tooth carrier to generate firing pulses for turning controlled switches ON and OFF. There can be only one modulating sinusoidal waveform in case of a single-phase inverter, or three for a three-phase inverter. On the other hand, SVM can only be applied to three-phase converters.

In SVM approach, a space vector defined as

$$\mathbf{V} = \frac{2}{3} \left(v_a(t) + v_b(t) e^{j2\pi/3} + v_c(t) e^{-j2\pi/3} \right) \quad (1)$$

is sampled at each sampling period T_s . It can be shown that this reference vector has a constant magnitude and rotates with the same speed as the angular frequency of phase quantities. A three-leg, two-level VSC (Fig. 1) can have eight distinct states of which six are active ones and the remaining two are inactive states that produce a zero line voltage. Tips of space vectors corresponding to these six active states point to vertices of a hexagon as shown in Fig. 2. Two null voltages, \mathbf{V}_0 and \mathbf{V}_7 lie at the origin. Space vectors and voltages corresponding to each state are shown in Table I.

TABLE I
EIGHT STATES OF A VSC AND CORRESPONDING SPACE VECTORS AND VOLTAGES

State	c, b, a	V	Pole Voltages, multiply by $V_{dc}/2$			Phase Voltages		
			V_{az}	V_{bz}	V_{cz}	V_{an}	V_{bn}	V_{cn}
0	000	$\mathbf{0}$	-1	-1	-1	0	0	0
1	001	$2V_{dc}/3 e^{j0}$	1	-1	-1	$2V_{dc}/3$	$-V_{dc}/3$	$-V_{dc}/3$
2	011	$2V_{dc}/3 e^{j\pi/3}$	1	1	-1	$V_{dc}/3$	$V_{dc}/3$	$-2V_{dc}/3$
3	010	$2V_{dc}/3 e^{j2\pi/3}$	-1	1	-1	$-V_{dc}/3$	$2V_{dc}/3$	$-V_{dc}/3$
4	110	$2V_{dc}/3 e^{j\pi}$	-1	1	1	$-2V_{dc}/3$	$V_{dc}/3$	$V_{dc}/3$
5	100	$2V_{dc}/3 e^{j4\pi/3}$	-1	-1	1	$-V_{dc}/3$	$-V_{dc}/3$	$2V_{dc}/3$
6	101	$2V_{dc}/3 e^{j5\pi/3}$	1	-1	1	$V_{dc}/3$	$-2V_{dc}/3$	$V_{dc}/3$
7	111	$\mathbf{0}$	1	1	1	0	0	0

Any space vector \mathbf{V} , which completely lies in the hexagon can be constructed by time averaging the adjacent two active space vectors and any zero vectors, as follows.

$$\mathbf{V}_{ref} = \frac{\mathbf{V}_n \times T_1 + \mathbf{V}_{n+1} \times T_2 + \mathbf{V}_0 \times T_0 + \mathbf{V}_7 \times T_7}{T_s} \quad (2)$$

This formula basically combines the two active vectors \mathbf{V}_n and \mathbf{V}_{n+1} (with shares of T_1 and T_2 , respectively) to come up with an approximation of the reference space vector valid only over the sampling period T_s . With the definition of modulation index as

$$m = \frac{V_{ref}}{V_{dc}/2} \quad (3)$$

Expression (2) can be solved for T_1 and T_2 as follows.

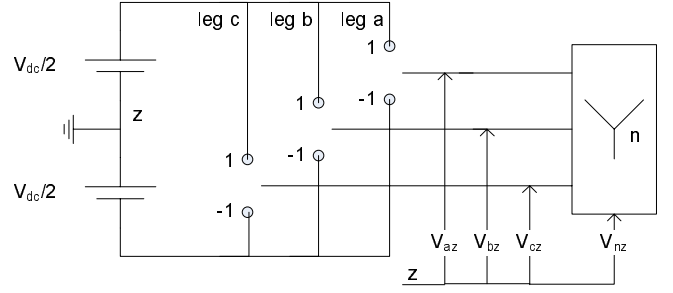


Fig. 1. Schematic diagram of a voltage source inverter.

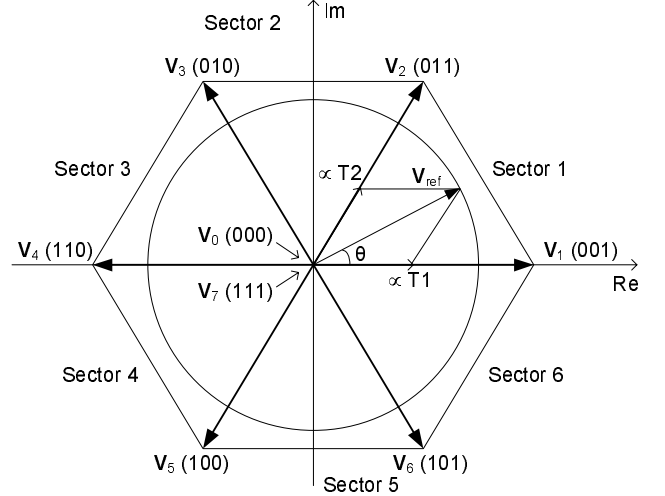


Fig. 2. Six active vectors and two null vectors in SVM.

*: State codes from left to right show the position of switches for leg c, leg b, and leg a, respectively.

$$T_1 = \frac{\sqrt{3}}{2} T_s m \sin(\pi/3 - \theta) \quad (4)$$

$$T_2 = \frac{\sqrt{3}}{2} T_s m \sin(\theta) \quad (5)$$

$$T_0 + T_7 = T_s - T_1 - T_2 \quad (6)$$

Applying active vectors and zero vectors for the periods given in (4) to (6), ensures that the average voltage has the same magnitude as desired. For each sampling period, space vectors can be applied in different sequences. For the first sector, one can use only one zero vector as in sequences **012**, **712**, **120**, and **127**; both zero vectors as in sequences **0127**, **7120**, **0217**, and **7210**; or two sequences back to back as in **01277210** for symmetry reasons.

To maintain three-phase and half-wave symmetry [7], the samples should be evenly distributed in each sector. Furthermore, the sequences used for each sample should be identical at corresponding positions within each sector. Needless to say, the number of samples used in each sector should be an integer number. Defining F_{sn} as

$$F_{sn} = \frac{F_s}{f} \quad (7)$$

where F_s is the sampling frequency and f is fundamental frequency of the waveform to be reconstructed (or equivalently V_{ref}), it should be an integer multiple of six as in (8)

$$F_{sn} = 6N \quad (8)$$

where N is the number of samples in a sector. N is an odd number in case of conventional implementation of SVM and even for bus clamping strategies. The conditions for retaining certain symmetries in each strategy have been studied in [7].

Although seemingly different, previous work has shown that PWM and SVM come from the same mathematical basics [8] and can be implemented with the same setup provided that correct modulating waveform is applied (for PWM) or correct arrangement of space vectors is selected (for SVM).

The fundamental difference between PWM and SVM lies in the fact that in PWM, switching times are directly determined based on the result of comparison, whereas in SVM, it is the duration of each switch state that is explicitly calculated (as can be seen in computations involved for determination of ON times of space vectors). In the context of space vectors and in conventional PWM, placement of space vectors is a direct consequence of comparison process; in SVM, however, the placement of active vectors within the sampling period (or carrier interval, in other terms) remains unspecified, which gives rise to an additional degree of freedom that can be used to achieve desired harmonic characteristics. The relationship between PWM and SVM is further investigated in [8], [9]. Another difference is that even without any provision for over-modulation the SVM has a wider linear region, which implies better utilization of dc bus voltage. Utilization of dc bus voltage can be further increased using certain overmodulation approaches, which are discussed in the following section.

III. OVERMODULATION STRATEGIES

Full utilization of dc link voltage has been a topic of extensive research. Overmodulation aims to increase the linear operation region of space vector modulators, and many methods have been developed over the years. These methods may or may not facilitate a smooth transition from overmodulation to square-wave operation.

Overmodulation starts when the reference vectors goes beyond the boundary defined by the hexagon formed by the tips of active space vectors. This occur for a modulation index larger than $2/\sqrt{3}$. At this point, reference vector touches the boundary at $\theta = \pi/6$. For a larger m , the average voltage cannot be constructed with a magnitude equal to the reference voltage and hence the waveform becomes distorted, which disturbs the linear characteristics between m and the magnitude of the fundamental component of output voltage. In other words, in the overmodulation region, the fundamental will not increase commensurately as m increases.

Several approaches to overmodulation have been proposed to extend the linear region of SVM. The overmodulation strategy proposed by Holtz *et al.* [10], which is also known as

two-zone approach, compensates for the magnitude of fundamental and hence increases dc bus voltage utilization and extends linear relationship at the expense of computational time and memory.

In zone I of this method, the trajectory of the reference vector is partly circular and partly on the hexagon. Up to a certain transition angle, it traces the part corresponding to actual m and after that, it continues to trace the hexagon boundary (Fig. 3.a). For boundary tracking region, the on-duration of zero vectors becomes zero. For this mode, the instantaneous value of modulation index is changed with reference vector angle so that the reference vector always remains in the hexagon. The transition from circular trajectory to boundary tracking is determined by transition angle, which depends on the desired value of modulation index [11] The maximum value of modulation index in this zone is 1.21 which occurs for zero transition angle.

While only the magnitude of reference voltage is distorted in zone I, both magnitude and angle are modified in zone II to achieve a higher m . In this zone (Fig. 3.b), the reference voltage is kept at a vertex for a particular time and then it is moved to hexagon boundary. This time is controlled by hold angle θ_h , which has a nonlinear relationship with m . The phase is then changed as

$$\theta' = \begin{cases} 0 & 0 \leq \theta \leq \theta_h \\ \frac{\theta - \theta_h}{\pi/6 - \theta_h} & \theta_h < \theta < \pi/3 - \theta_h \\ \pi/3 & \pi/3 - \theta_h \leq \theta \leq \pi/3 \end{cases} \quad (9)$$

Transition to square-wave operations completes when θ_h becomes equal to $\pi/6$.

A much simpler overmodulation approach that also uses the concept of hold angle is suggested by Bolognani *et al.* [11]. In this method, which is also known as one-zone approach, a single algorithm is used for the whole range of overmodulation. This is done by defining a hold angle, which is the angle corresponding to the intersection of the hexagon boundary and circular trajectory of the reference voltage. The reference vector will be produced as long as possible. As soon as reference vectors goes beyond hexagon which occurs for $\theta > \theta_h$ a voltage vector of same amplitude but with a modified phase is produced. The phase is kept at the hold angle until θ reaches $\pi/6$. From $\pi/6$ to $\pi/3 - \theta_h$, the phase is held at $\pi/6 - \theta_h$. This is shown in Fig. 4. The modified angle is defined in (10).

$$\theta' = \begin{cases} \theta & 0 \leq \theta < \theta_h \\ \theta_h & \theta_h \leq \theta < \pi/6 \\ \pi/3 - \theta_h & \pi/6 \leq \theta < \pi/3 - \theta_h \\ \theta & \pi/3 - \theta_h \leq \theta < \pi/3 \end{cases} \quad (10)$$

Square-wave operation is achieved for θ_h equal to zero.

As it can be seen, this method is much simpler in implementation than the two-zone approach but has a higher harmonic content. It can be argued, however, that with fewer computations the processor load is decreased and therefore, switching frequency can be further increased, which offsets

the poor harmonic spectrum. The characteristics of overmodulation strategies has been further investigated in [13]–[16] and their Fourier analysis is studied in [17].

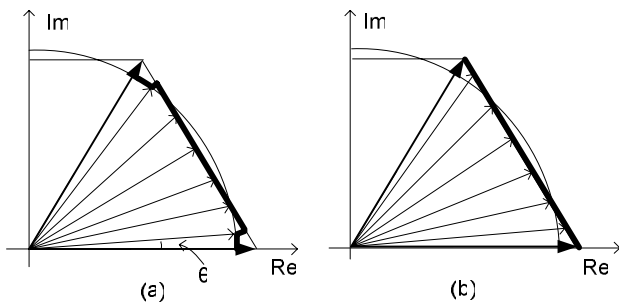


Fig. 3. Two-zone overmodulation approach, (a) zone I, (b) zone II.

*: Black parts are the actual trajectory of constructed voltage.

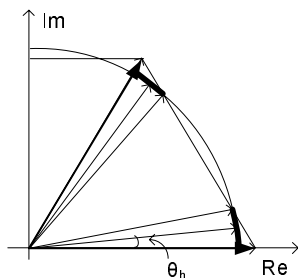


Fig. 4. One-zone approach to modulation.

*: Black parts are the actual trajectory of constructed voltage.

IV. TRANSIENT MODELING AND SIMULATION RESULTS

Transients are inevitable events in all power systems and industrial drives. They can be initiated by a wide array of causes ranging from planned operation-time adjustments (such as changes in the set-point of a generator) to unplanned faults and external disturbances. Short-term transients in power systems are best modeled in a transient simulation program, in which detailed models of systems components can be assembled to form a network and exact time-domain solution methods are used to solve the resulting system.

Since the switches in a VSC are turned ON and OFF very rapidly, they do generate high-frequency voltage and current components that propagate through the network. A transient simulation program is thus a suitable host for modeling and simulation of such high-frequency transients.

In [18] a software implementation of SVM using both Matlab/Simulink and PSim is presented. Although the work provides a means to study SVM-based generated waveforms, it does not cover the overmodulation region.

In this section a transient simulation model of an SVM-controlled VSC is developed (Fig. 5). The model is implemented in the PSACD/EMTDC electromagnetic transient simulation program [19]. The developed model does include the linear and overmodulation modes of operation; moreover, it allows the user to select sampling frequency and other

parameters according to their design requirements.

At each instant of time, this component generates three required firing pulses for upper switches. The other three pulses for bottom switches can be obtained simply by inverting the former three ones.

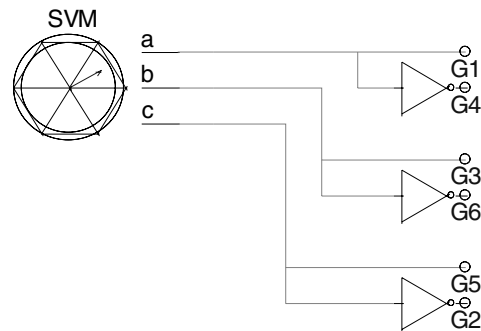


Fig. 5. Developed SVM component with minimum connections.

The firing commands are generated in such a way that they provide three-phase symmetry (3PS), half-wave symmetry (HWS), and quarter-wave symmetry (QWS). The first two symmetries eliminate triple- n and even harmonics from line voltage, respectively. Firing pulses are used to drive the switches of a VSC as shown in Fig. 6. A balanced star-connected RL load with isolated neutral is connected to VSC. The load and dc source parameters are shown in Table II.

The proposed model is used to simulate the operation both in linear and nonlinear regions with $m = 0.8$ and $m = 1.2$, respectively. The sampling frequency for both simulations is kept at $F_{sn} = 48$.

Although normally low-order harmonics are analyzed for a study on harmonic characteristics, as in IEEE Standard 519 [20], harmonics up to 63 are used for calculation of WTHD.

A. Voltage and Current Waveforms

Fig. 7.a shows the generated line voltage for $m = 0.8$. It is evident that the line voltage passes QWS (and so, HWS). This efficiently eliminates even harmonics. Two other curves, Fig. 7.b and Fig. 7.c show pole voltage and phase voltage, respectively. As shown in Table I, the pole voltage alternates between $+V_{dc}$ and $-V_{dc}$, while the phase voltage can assume values of $\pm 2V_{dc}/3$ and $\pm V_{dc}/3$.

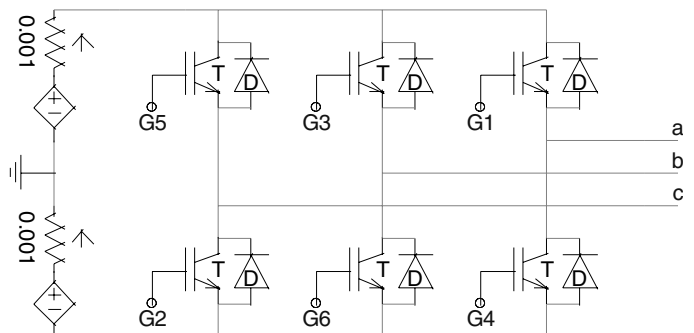


Fig. 6. A three-leg two-level VSC model in PSCAD.

TABLE II
LOAD PARAMETERS

V_{dc} (V)	V_{rated} (V)	f (Hz)	R (Ω)	L (mH)
400	140	60	10	13

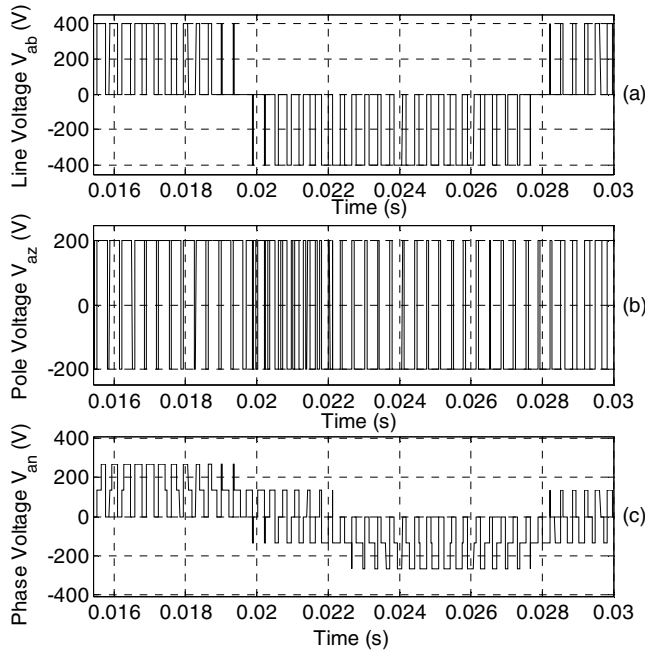


Fig. 7. Generated (a) line voltage (b) pole voltage (c) phase voltage, $F_{sn} = 48$, $m = 0.8$.

Fig. 8 shows the line current. Because of the inductive nature of the load, higher-order harmonics have been filtered out and the current waveform is sinusoidal in essence.

Results for overmodulation using one-zone approach are also shown. Fig. 9.a shows the line voltage. It is clear that the waveform still possesses QWS. Fig. 9.b and Fig. 9.c show pole and phase voltages, respectively.

Fig. 10 shows the line current. The current waveform has deviated from sinusoidal shape, which is expected because the reference voltage is no longer sinusoidal.

B. Harmonic Content

Fig. 11 shows the harmonic spectrum of pole voltage for $m = 0.8$. As can be seen, except for the third harmonic the first group of harmonics has been shifted to around the 48th harmonic. Because of HWS, even harmonics are not present in the pole voltage.

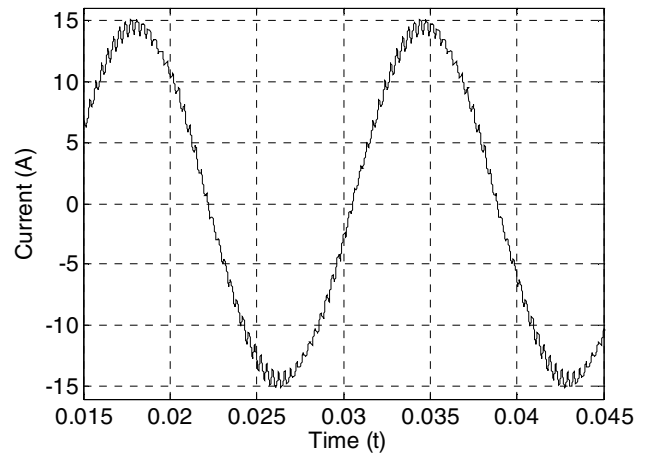


Fig. 8. Line current, $F_{sn} = 48$, $m = 0.8$.

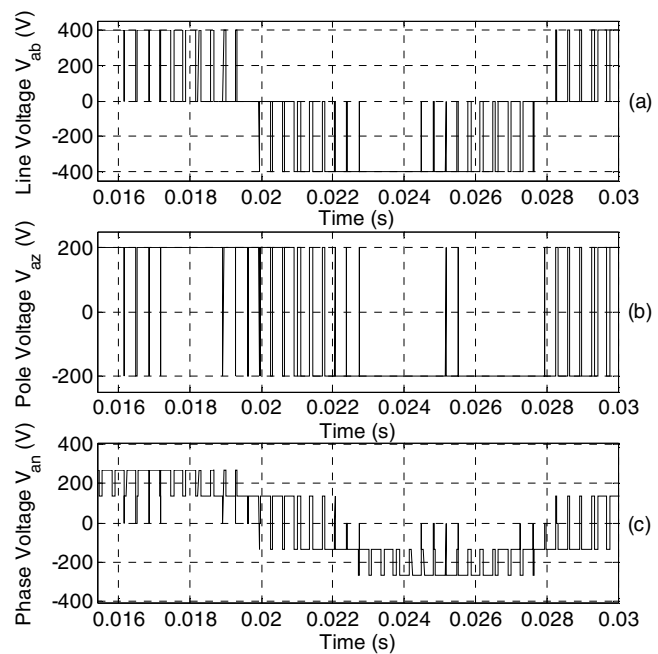


Fig. 9. Generated (a) line voltage (b) pole voltage (c) phase voltage, $F_{sn} = 48$, $m = 1.2$.

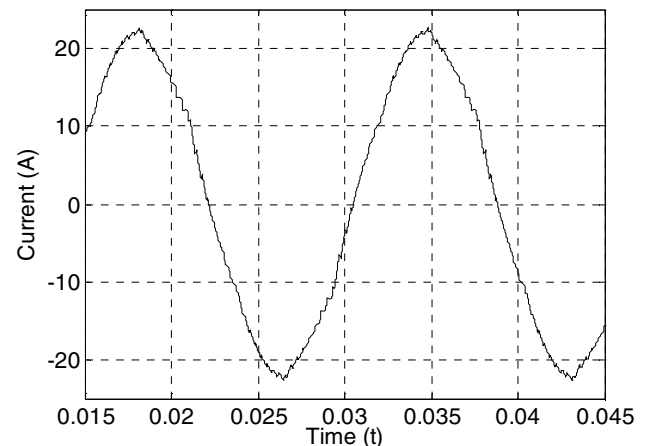


Fig. 10. Line current, $F_{sn} = 48$, $m = 1.2$.

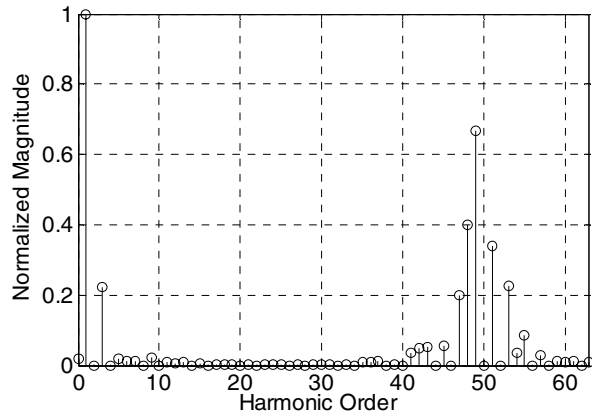


Fig. 11. Harmonic spectrum for the first 63 harmonics of pole voltage, $F_{sm}=48$, $m=0.8$.

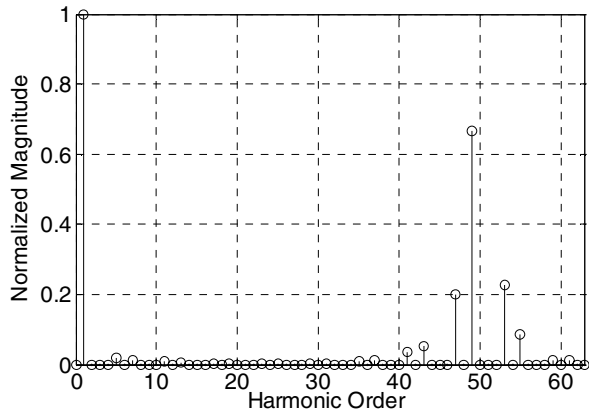


Fig. 12. Harmonic spectrum for the first 63 harmonics of line voltage, $F_{sm}=48$, $m=0.8$.

As load only sees the line voltage, it is worthwhile to study it in more detail. Even-numbered harmonics are further decreased in the line voltage as shown in Fig. 12. Due to 3PS, triple- n harmonics are totally absent from the line voltage. Weighted THD calculated for first 63 harmonics is as low as 1.58%.

Fig. 13 shows the harmonic spectrum of the pole voltage for $m = 1.2$. Still the third harmonic is the most significant harmonic present in the waveform but the magnitude of other low order harmonics has been increased. In Fig. 14 it is shown that similar to operation in linear mode, line voltage has lower harmonics and even and triple- n harmonics do not exist.

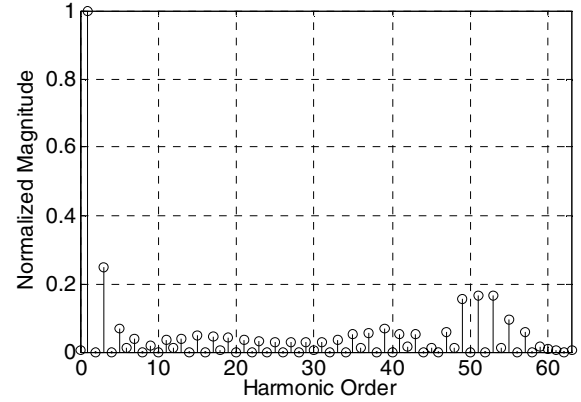


Fig. 13. Harmonic spectrum for the first 63 harmonics of pole voltage, $F_{sm}=48$, $m=1.2$.

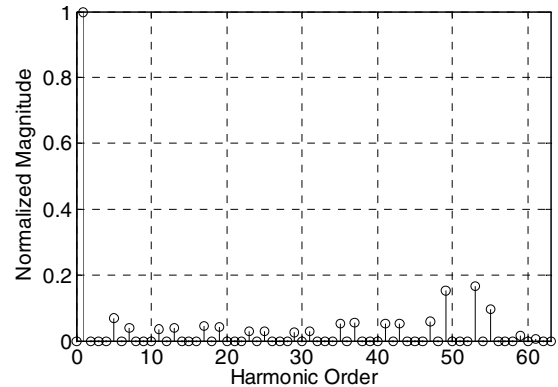


Fig. 14. Harmonic spectrum for the first 63 harmonics of line voltage, $F_{sm}=48$, $m=1.2$.

The magnitude of the constructed pole voltage is 237.3 as obtained by FFT block. Note that if the linear mode of operation could have extended to $m = 1.2$, a pole voltage of 240 V was to be obtained. However, since we are actually operating in the nonlinear range, an actual voltage of 237.7 V is obtained. Note that this is a match of over 98.8%, which is due to compensation in the overmodulation range.

In practice the factors that could contribute to the deviations of the actual values from their theoretically expected values include inherent uncertainties in parameter values, fluctuations in dc bus voltage, and numerical round-off errors.

Weighted THD is increased to 1.69%.

Table III compares normalized line voltage harmonic magnitudes for $m = 0.8$ and $m = 1.2$. While still due to symmetries in waveform even and triple- n harmonic are absent for overmodulation region, other harmonics are increased.

TABLE III
COMPARISON OF NON-ZERO HARMONICS IN LINE VOLTAGE

Harmonic Order	$m = 0.8$	$m = 1.2$
5	1.8415	6.7275
7	1.103	3.9141
11	0.8321	3.5441
13	0.6693	3.6921

17	0.3275	4.6432
19	0.0875	4.1805
23	0.0137	3.0015
25	0.0877	2.8877
29	0.2708	2.6695
31	0.2208	2.9266

*: Harmonic values are in percentage of the fundamental.

V. CONCLUSION

In this paper, a digital implementation of space vector modulation in an electromagnetic transient simulation program has been proposed, which can be used for the study of power systems with embedded power electronics. The developed model incorporates both linear and nonlinear (overmodulation) regions of the operation. Since the model is developed in a transient simulation program, it allows detailed simulation of short-term and transient phenomena in power systems and industrial motor drives, where SVM-modulated converters are deployed; moreover, harmonic analysis of the voltage and current waveforms becomes possible, which yields invaluable information about the harmonic spectrum as well as filtering requirements. Since the model allows the user to set the sampling rate and other relevant parameters, it enables parametric studies involving variations of those parameters.

Simulation results reported in the paper confirm that the developed model generates waveforms with complete symmetry in both linear and nonlinear regions. The harmonic content of the waveforms could be controlled and centered around high-frequency components, resulting in less intense filtering requirements.

REFERENCES

- [1] H. W. Van der Broeck, H. C. Skudelny, and G. Stanke, "Analysis and realization of a pulsewidth modulator based on voltage space vectors," *IEEE Trans. Industry Applications*, vol. 24, pp. 142–150, Jan./Feb. 1988.
- [2] J. Holtz, "Pulsewidth modulation—a survey," *IEEE Trans. Industrial Electronics*, vol. 39, no. 5, pp. 410–420, Oct 1992.
- [3] D. G. Holmes, "The significance of zero space vector placement for carrier-based PWM schemes," *IEEE Trans. Industry Applications*, vol. 32, no. 5, pp. 1122–1129, Sept.–Oct. 1996.
- [4] G. Narayanan and V. T. Ranganathan, "Two novel synchronized bus-clamping PWM strategies based on space vector approach for high power drives," *IEEE Trans. Power Electronics*, vol. 17, no. 1, pp. 84–93, Jan. 2002.
- [5] R. Jobing, F. S. van der Merwe, and M. J. Kamper, "Digital implementation of bus clamped space vector modulation," *IEEE Trans. Energy Conversion*, vol. 9, no. 2, pp. 334–348, June 1994.
- [6] F. Jenni and D. Wueest, "The optimization parameters of space vector modulation," *Fifth European Conf. Power Electronics and Applications*, vol. 4, pp. 376–381, 13–16 Sept. 1993.
- [7] G. Narayanan and V. T. Ranganathan, "Synchronized PWM strategies based on space vector approach: I. Principles of waveform generation," *IEEE Proc. Electric Power Applications*, vol. 146, no. 3, pp. 267–275, May 1999.
- [8] D. G. Holmes, "The general relationship between regular-sampled pulse-width-modulation and space vector modulation for hard switched

- converters," *Conf. Record of 1992 IEEE Industry Application Society Annual Meeting*, vol. 1, pp. 1002–1009, 4–9 Oct. 1992.
- [9] Keliang Zhou and Danwei Wang, "Relationship between space-vector modulation and three-phase carrier-based PWM: a comprehensive analysis [three-phase inverters]," *IEEE Trans. Industrial Electronics*, vol. 49, no. 1, pp. 186–196, Feb. 2002.
- [10] J. Holtz, A. M. Khambadkone, and W. Lotzkatz, "On continuous control of PWM inverters in the overmodulation range including the six-step mode," *IEEE Trans. Power Electronics*, vol. 8, no. 4, pp. 564–554, Oct. 1993.
- [11] A. R. Bakhshai, G. Joos, and P. K. Jain, "Incorporating the overmodulation range in space vector pattern generators using a classification algorithm," *IEEE Trans. Power Electronics*, vol. 15, no. 1, pp. 83–91, Jan. 2000.
- [12] S. Bolognani and M. Zigliotto, "Novel digital continuous control of SVM inverters in the overmodulation range," *IEEE Trans. Industry Applications*, vol. 33, no. 2, pp. 525–530, March–April 1997.
- [13] G. Narayanan and V. T. Ranganathan, "Extension of operation of space vector PWM strategies with low switching frequencies using different overmodulation algorithms," *IEEE Trans. Power Electronics*, vol. 17, no. 5, pp. 788–798, Sept. 2002.
- [14] Lee Dong-Choon and G-Myoung, "A novel overmodulation technique for space-vector PWM inverters," *IEEE Trans. Power Electronics*, vol. 13, no. 6, pp. 1144–1151, Nov. 1998.
- [15] G. Narayanan and V. T. Ranganathan, "Overmodulation algorithm for space vector modulated inverters and its application to low switching frequency PWM techniques," *IEEE Proc. Electric Power Applications*, vol. 148, no. 6, pp. 521–536, Nov. 2001.
- [16] Hee-Jhung Park and Myung-Joong Youn, "A new time-domain discontinuous space-vector PWM technique in overmodulation region," *IEEE Trans. Industrial Electronics*, vol. 50, no. 2, pp. 349–355, April 2003.
- [17] S. Bolognani and M. Zigliotto, "Space Vector Fourier analysis of SVM inverters in the overmodulation range," *Proc. Int'l Conf. on Power Electronics, Drives, and Energy Systems for Industrial Growth*, vol. 1, pp. 319–324, Jan. 1996.
- [18] D. Rathnakumar, J. LakshmanaPerumal, and T. Srinivasan, "A new software implementation of space vector PWM," *IEEE Proc SoutheastCon 2005*, pp. 131–136, 8–10 April 2005.
- [19] *EMTDC Manual*, Manitoba HVDC Research Centre Inc., April 2004.
- [20] *IEEE Recommended Practices and Requirements for Harmonic Control in Electrical Power Systems*, IEEE Standard 519, 1992.



Ali Mehrizi-Sani (S'05) obtained a B.Sc. in electrical engineering from Sharif University of Technology, Tehran, Iran and a B.Sc. in petroleum engineering from Sharif University of Technology and Petroleum University of Technology, Ahwaz, Iran both in 2005. He is currently pursuing his studies at Master's level in electrical engineering at the University of Manitoba.

His areas of interest include power electronics, electric machines modeling and design, and power system analysis and simulation. He is currently working on advanced switch and converters control methodologies.

Mr. Mehrizi-Sani is also a member of Power Engineering Society of IEEE and Society of Petroleum Engineers.



Shaahin Filizadeh (M'04) obtained his B.Sc. and M.Sc. degrees both in electrical engineering from Sharif University of Technology. He obtained his Ph.D. degree (in 2004) from the Department of Electrical and Computer Engineering, University of Manitoba, where he currently holds an Assistant Professor position. His areas of interest include power systems simulations, applications of power electronics in power systems, and nonlinear optimization.